THE JOURNAL OF PHYSICAL CHEMISTRY B

Article

pubs.acs.org/JPCB

Cyclodextrin-Scaffolded Alamethicin with Remarkably Efficient Membrane Permeabilizing Properties and Membrane Current Conductance

Claudia U. Hjørringgaard,[†] Brian S. Vad,[‡] Vladimir V. Matchkov,[§] Søren B. Nielsen,[‡] Thomas Vosegaard,[†,∥] Niels Chr. Nielsen,*[,†] Daniel E. Otzen,*[,‡] and Troels Skrydstrup*[,†]

[†]Center for Insoluble Protein Structures (inSPIN), Interdisciplinary Nanoscience Center (iNANO) and Department of Chemistry, Aarhus University, Langelandsgade 140, DK-8000 Aarhus C, Denmark

[‡]Center for Insoluble Protein Structures (inSPIN), Interdisciplinary Nanoscience Center (iNANO) and Department of Molecular Biology, Aarhus University, Gustav Wieds Vej 10C, DK-8000 Aarhus C, Denmark

[§]Department of Biomedicine, Aarhus University, Ole Worms Allé 6, 8000 Aarhus, Denmark

[∥]Aarhus University School of Engineering, Langelandsgade 140, DK-8000 Aarhus C, Denmark

Supporting Information

ABSTRACT: Bacterial resistance to classical antibiotics is a serious medical problem, which continues to grow. Small antimicrobial peptides represent a potential solution and are increasingly being developed as novel therapeutic agents. Many of these peptides owe their antibacterial activity to the formation of trans-membrane ion-channels resulting in cell lysis. However, to further develop the field of peptide antibiotics, a thorough understanding of their mechanism of action is needed. Alamethicin belongs to a class of peptides called peptaibols and represents one of these antimicrobial peptides. To examine the dynamics of assembly and to facilitate a thorough structural evaluation of the alamethicin ion-channels, we have applied click chemistry for the synthesis of templated alamethicin multimers covalently attached to cyclodextrin-scaffolds. Using oriented circular dichroism, calcein release assays, and single-channel current measurements, the α-helices of the templated multimers were demonstrated to insert into lipid bilayers forming highly efficient and remarkably stable ion-channels.

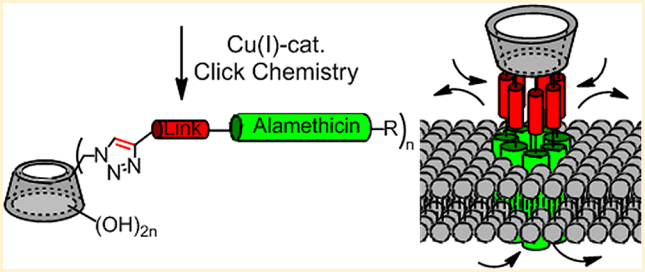

1. INTRODUCTION

Antimicrobial peptides (AMPs) represent a class of potential antibiotics, which are found among all classes of life as part of the innate immune response against fungi, viruses, and both Gram-positive and Gram-negative bacteria.[1−8] Most of the AMPs disrupt the bacterial membrane leading to cell lysis, making it difficult for the bacteria to develop resistance against these peptides, in contrast to conventional small-molecule antibiotics, which have very specific binding sites affecting cellular metabolism. The two main common membrane-disrupting models of the AMPs are the carpet and pore-formation mechanisms; the latter is subdivided into barrel-stave and toroidal pore mechanisms.[4,9−14]

Peptaibols, a subclass of the antimicrobial peptides isolated from fungi, have gained much interest lately due to their antimicrobial activity.[8,15−17] The most frequently studied peptaibol is the 19-residue peptide, alamethicin (Alm), which is acetylated at the N-terminus and extended with phenylalaninol at the C-terminus (Figure 1).[18−23] Alamethicin has an α-helical conformation prompted by its high content of the helix-inducing aminoisobutyric acid (Aib) residue.[24] While it is well-established that this hydrophobic α-helical peptide exerts its biological effect via oligomerization and channel formation in the membrane

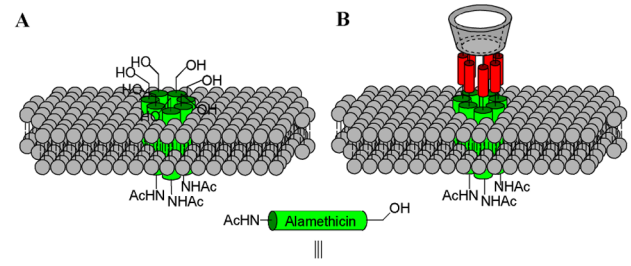

Figure 1. Schematic representations of an alamethicin ion-channel formed by (A) alamethicin monomers and by (B) alamethicin:cyclodextrin conjugate linked at the C-terminal.

(Figure 1A), the precise molecular structure of these pores still remains speculative,[25−36] but recent NMR and MD investigations suggest that they are highly dynamic and nonuniform by nature.[37−41]

Received: October 13, 2011
Revised: June 6, 2012
Published: June 7, 2012

   dx.doi.org/10.1021/jp2098679 | J. Phys. Chem. B 2012, 116, 7652−7659

Much effort has already been made to prepare and study chemically linked alamethicin analogues as dimers or with linear or cyclic-scaffolds.[42−55] Both dimers and conjugates containing 3−5 alamethicins were shown to form ion-channels with increased lifetime. Stabilization of the ion-channel has also been reported for noncovalently linked alamethicin analogues applying a Leu-zipper,[55,56] fullerene attachment,[57] or divalent metal-chelation.[50,58] Previous dimer studies indicate that the most stable and predominant channel structure consist of 6−8 helices,[43,45,48,54] as also suggested from studies based on NMR spectroscopy[27] and MD simulations.[29] However, only conjugates mimicking lower oligomerization states, 3−5 helices, have been reported. Applying the template assembled synthetic protein (TASP) approach[59,60] by covalently tethering alamethicin to a suitable cyclic template such as cyclodextrin (CD) (Figure 1B) would create larger conjugates mimicking these predominant oligomerization states, 6−8 helices. These conjugates could lead to more stable membrane channels, which are uniform in structure and therefore possibly more active than the free monomer, in particular at lower concentrations. Furthermore, these conjugates could provide suitable models for solid-state NMR studies of membrane channels composed of a predefined number of peptide units.

In this article, we report on the synthesis of a new class of templated alamethicins exploiting the full length peptides conjugated to α- and β-cyclodextrins from the C- or N-terminal, which can be assembled using click chemistry.[61−65] These templated AMPs, containing up to 7 alamethicins, possess the same membrane-induced structure as alamethicin according to circular dichroism but display remarkably improved efficacy of membrane permeabilization and ion-channel stability, compared to the nontemplated peptide, as determined by calcein-release experiments and single-channel current measurements, respectively. These results suggest that the combination of antimicrobial peptides with a cyclodextrin-scaffold is ideal for inducing stable membrane channel formation.

2. EXPERIMENTAL SECTION

2.1. General Procedure for the Cu(I)-Catalyzed Alkyne−Azide Cycloaddition (CuAAC) Using Optimized Conditions. The azide was dissolved in dry DMF (0.01 M) under an atmosphere of argon. The alkyne (1.1 equiv of pr. azide) and Et_3N (20 equiv) were added, and the reaction mixture was deoxygenated by bubbling through with argon for 15 min. CuI (20 mol % according to the alkyne) was added and the reaction mixture was heated to 70 °C and stirred for 4−20 h (see Supporting Information for the specific reaction time). Quadrapure IDA resins (0.16 mmol/g) were added and shaken overnight. The resins were filtered off, and the reaction mixture evaporated in vacuo. The crude product was dissolved in 1:1 MeCN/NH_3 (aq. 2.5%), lyophilized, and purified by RP-HPLC or gel filtration chromatography.

2.2. Oriented Circular Dichroism. Alamethicin or alamethicin:cyclodextrin conjugates were dissolved in 80:20 acetonitrile/H_2O to a final concentration of 10 mg/mL. Peptide solutions were mixed with DOPG to a final concentration of 10 mg/mL lipid and 0.5 mg/mL peptide in 1:1 chloroform/methanol. Samples were spotted on quartz cuvette and dried in a vacuum desiccator, leading to membrane multilayers. Dry multilayer membranes were rehydrated overnight in a humidity chamber equilibrated at 98% relative humidity (RH) in the presence of a saturated K_2SO_4 salt solution. Circular dichroism spectra were obtained with the incident light perpendicular to the membrane plane using a synchrotron radiation source. Spectra were normalized at the red-shifted minimum.[66]

2.3. Solution Circular Dichroism. Circular dichroism studies were performed using parameters previously described.[67] All experiments were carried out in 20 mM Tris-HCl pH 8.0, at 25 °C using a 1 mm quartz cuvette. Alamethicin or alamethicin:CD conjugates were mixed with lipid and incubated for 1 h before spectra were recorded. Buffer contributions (including lipid) were subtracted.

2.4. Calcein Dye Leakage Experiments. These were performed as described previously.[67] LUVs (large unilamellar vesicles) containing calcein were prepared using desiccated lipids, which were resuspended by vortexing. The samples were exposed to at least seven cycles of freezing and thawing before extrusion through a 200 nm pore filter. Free calcein was removed by gel filtration, and the vesicles were diluted to a final concentration of 16 μM in 50 mM tris pH 7.5. To monitor the release of free calcein from the vesicles and the concomitant rise in fluorescence, the solution was excited at 490 nm, measuring emission at 515 nm every second during and after peptide injection. Spectra were normalized with regards to maximum fluorescence using the equation

$$\text{Dye leakage}\ (\%) = 100 \times (F - F_0)/(F_t - F_0)$$

where F is the fluorescence intensity achieved by the peptides, and F_0 and F_t are fluorescence intensities without the peptides and with the addition of Triton X-100, respectively.

2.5. Voltage Clamp Studies. Channel-forming activity induced by the Alm:CD conjugates was assayed in a voltage clamp study. The tip-dip method has been used to isolate bilayers onto the tip of micropipets as described previously.[68] Shortly, lipid membrane was formed from DOPG dissolved in *n*-hexane (10 mg/mL). The solvent was evaporated and formation of bilayers at the glass patch pipet tip was achieved by repeatable lowering and raising back the pipet through the lipid monolayer on the bath surface. Bilayer formation was indicated by increasing tip resistance to ~1 GΩ. Data acquisition and analysis were done with the software packages Clampex7 for Windows (Axon Instruments, Inc.). The data have been sampled at 10 kHz with a digital filter of 0.01 kHz. For plotting purposes, the data were filtered with data reduction by decimation. Experiments were conducted at room temperature (22−24 °C). An equal electrolyte composition was used for the bath and the pipet solutions (in mM): 150 KCl; 2 HEPES; 10^{-3} $CaCl_2$; pH 7.3 adjusted with KOH.

3. RESULTS AND DISCUSSION

3.1. Synthesis of the Peptide:Cyclodextrin Conjugates. The choice of the cyclodextrin-scaffold for these studies was made on the basis of the different ring sizes available in bulk quantities for cyclic oligosaccharides containing from 6 to 8 glucose units (α-, β-, and γ-CD), and the ease of selective modification of the primary C6-hydroxyl group of the individual glucose units.[69] Alamethicin:CD conjugates varying in the number of peptides from 6 to 8 (as well as higher ratios for less abundant higher-size CDs) are therefore in principle accessible with this scaffold class. CDs have furthermore previously been used as both channel templates[70−73] and channel modulators.[74−78]

Covalent linking of the peptide to CD was conceived to proceed by a known transformation of the C6-hydroxyl groups to the corresponding azides[79−81] followed by a Cu-catalyzed cycloaddition with an alkyne conjugated alamethicin possessing an alkyne linker. The synthesis of the alkyne-containing linker

dx.doi.org/10.1021/jp2098679 | J. Phys. Chem. B 2012, 116, 7652−7659

covalently attached to either the N-terminal or the C-terminal end of alamethicin using a combination of solid-phase peptide synthesis and solution phase chemistry is depicted in Scheme 1.

Scheme 1. Synthesis of the Alkyne-Containing Linker Attached to the Peptide at (A) the C-Terminal and (B) the N-Terminal

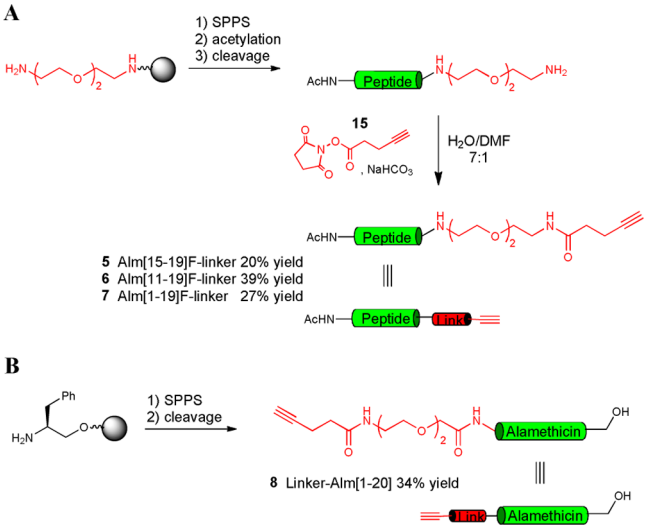

For the C-terminal functionalization, the synthetic route commenced with the trityl resin preloaded with bis-(aminoethyl)ethylene glycol (Scheme 1A). We have recently reported a fully automated solid-phase synthesis of peptaibols exploiting both microwave and double coupling of amino acids positioned after an α,α-dialkylated amino acid.[82] This methodology allowed us to rapidly prepare the resin bound alamethicin in which the phenylalaninol unit was replaced by phenylalanine. Subsequent TFA-mediated liberation of the peptide with the linker from the resin and further functionalization of the primary amine with *N*-succinimidyl-4-pentynoate completed the synthesis of the alkyne-linked alamethicin. Two truncated versions of the peptaibol were also prepared as shown with compounds **5** and **6** containing, respectively, the amino acid residues 15−19 and 11−19 of alamethicin. These were synthesized as model systems for the conjugation studies and also for investigations of the channel-forming properties of the shortened peptide derivatives.

The N-terminally linked alamethicin variant was prepared by a fully automated synthesis starting from the Cl-trityl resin preloaded with phenylalaninol (Scheme 1B). Subsequent peptide coupling to install the full alamethicin structure was followed by double coupling of 8-(9-fluorenylmethyloxycarbonyl amino)-3,6-dioxaoctanoic acid under standard conditions, liberation of the primary amine and coupling with pentynoic acid. Cleavage from the resin with TFA provided the desired alkyne:peptide conjugate in acceptable yields.

Considerable efforts were made to identify suitable reaction conditions for effectively promoting the Cu(I)-catalyzed alkyne−azide cycloaddition (CuAAC) for assembling the alamethicin:cyclodextrin conjugates. The best reaction conditions were found using 20 mol % CuI and excess triethylamine in dry DMF at 70 °C as shown in Scheme 2. The results of the CuAAC are depicted in Table 1. While the cycloadditions with the alkynes **5** and **6** (entries 1 and 2) were finished after 4 h, the same reactions with the full-length alamethicin:alkynes, to either

Scheme 2. Optimized CuAAC Conditions

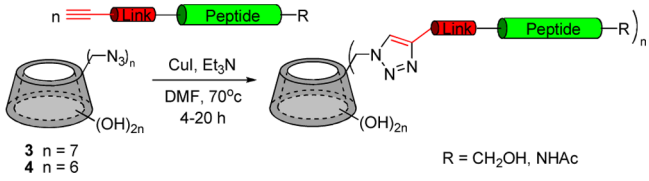

Table 1. CuAAC between the Alkyne Containing Peptides and the Azido CD-Scaffolds

entry	CD-scaffold	alkyne	time	product (yield)
1	3	5	4 h	9 (51%)[a]
2	3	6	4 h	10 (46%)[a]
3	3	7	o/n[b]	11 (49%)[c]
4	4	7	o/n[b]	12 (60%)[c]
5	3	8	20 h	13 (89%)[c]
6	4	8	20 h	14 (86%)[c]

[a]Isolated yields after RP-HPLC purification. [b]o/n = overnight. [c]Isolated yields after gel filtration chromatography.

the modified α- or βCD required longer reaction times for completion (entries 3−6).

To remove the copper ions, the metal scavenging resin Quadrapure IDA was then added. Purification of the synthesized conjugate was accomplished by semipreparative reverse-phase HPLC and the compounds were characterized by MALDI-TOF MS. HPLC purification of the full-length conjugates linked at the C-terminal, Alm$C\alpha$CD and Alm$C\beta$CD, or at the N-terminal, Alm$N\alpha$CD and Alm$N\beta$CD, with molecular weights reaching up to 16.6 kDa was not suitable. However, this could be accomplished by gel filtration chromatography providing the desired macromolecules. Characterization of conjugates by MALDI-TOF MS revealed that these compounds also contained to a certain extent CD conjugates with one less peptide (see Supporting Information); however, the peptides were estimated to be of purity of greater than 80%. Furthermore, and dependent on the structure of the conjugate, one to four copper ions were included in the detected compounds (see Supporting Information). This is most likely related to the large size and the compactness of the structures, which impedes copper extraction and the high content of triazoles that can act as ligands for copper. Nevertheless, we assumed that these modifications would not influence the overall assessment of the membrane permeabilizing properties of these alamethicin:CD conjugates.

3.2. Conformational Studies in Solution and Vesicles.

Coupling of alamethicin to a scaffold could be expected to impart lower flexibility and fewer conformational degrees of freedom when interacting with membranes. We used far-UV circular dichroism to follow the changes in the secondary structure of alamethicin alone and the various conjugates when exposed to the zwitterionic lipid dioleoyl-phosphatidyl choline (DOPC).

Qualitatively similar results were obtained with vesicles containing 80% DOPC + 20% of the anionic lipid dioleoyl-phosphatidyl glycerol (DOPG). In solution, alamethicin and alamethicin with only the alkyne-linker show minima of equal magnitude at 205 and 225 nm but undergo a large spectroscopic change upon binding to DOPC, leading to a deep minimum at 222−226 nm and a shoulder at 208 nm (shown for alamethicin in Figure 2A). A similar spectroscopic change has previously been reported for alamethicin.[83,84] In contrast, the four full-length

dx.doi.org/10.1021/jp2098679 | J. Phys. Chem. B 2012, 116, 7652−7659

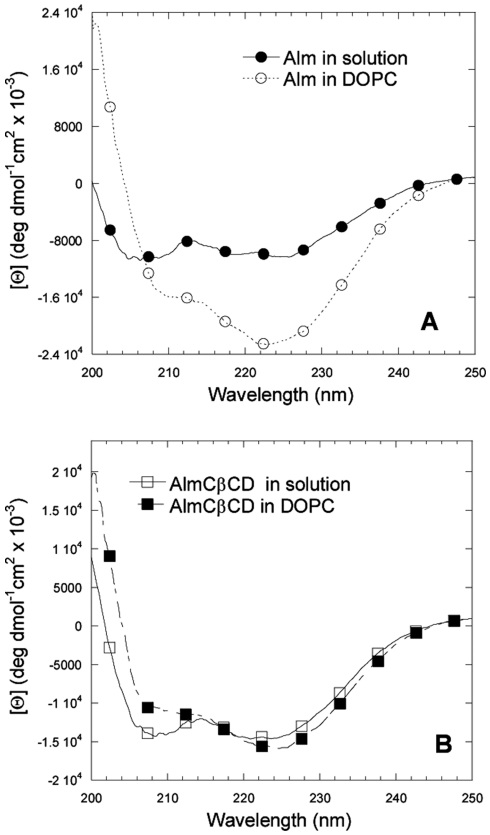

Figure 2. Circular dichroism spectra of (A) alamethicin and (B) alamethicin-βCD conjugate linked at the C-terminal in the presence and absence of 1 mM 200 nm unilamellar vesicles. (C) Comparison of the ellipticity of Alm and AlmCβCD at different DOPC concentrations.

alamethicin:CD conjugates AlmCαCD, AlmCβCD, AlmNβCD, and AlmNαCD only show minor changes upon switching from solution to DOPC (shown for AlmCβCD in Figure 2B).

The solution spectra of these constructs are more similar to their lipid spectra than to the solution spectrum of alamethicin, indicating that the scaffolding has induced a structure that is similar to the lipid-state. This may be seen more clearly in Figure 2C where the ellipticities at the two minima 208 and 222 nm are plotted versus increasing DOPC concentration. The ellipticity changes are clearly smaller for scaffolded than for free alamethicin, although the titration is completed at roughly the same lipid concentration for both constructs, indicating an essentially unaltered lipid affinity.

To probe the orientation of the peptides in the lipid, we recorded oriented circular dichroism spectra of free and scaffolded alamethicin in multilayer membranes composed of DOPG lipids under conditions of controlled humidity (98% RH) at a peptide to lipid molar ratio of 1 to 50.[85,86] With this technique, it is possible to distinguish between helical orientations predominantly parallel and perpendicular to the membrane plane since the orientation parallel to the membrane gives rise to a negative signal at ~208 nm, which is much less pronounced in the perpendicular orientation.[87] The C-terminally linked alamethicin conjugates, AlmCαCD and AlmCβCD, showed a pronounced maximum around 201 nm just as alamethicin at 98% RH (though slightly diminished in intensity), indicative of Alm helices, which on average are perpendicular to the membrane plane (rather than parallel) similar to alamethicin (Figure 3). For the N-terminally linked

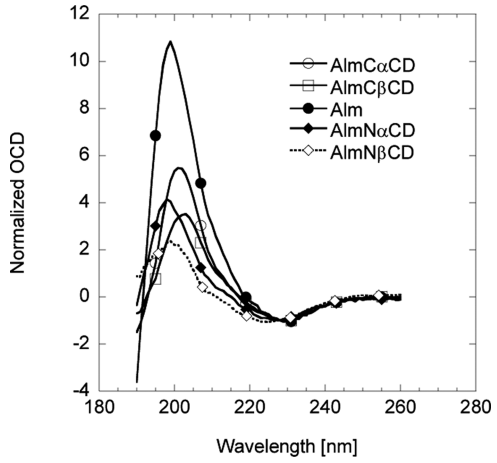

Figure 3. Oriented circular dichroism spectra of alamethicin and alamethicin:CD conjugates in DOPG multilayer membranes at 98% RH.

AlmNβCD and AlmNαCD, the presence of a more pronounced shoulder around 208 nm and the slightly red-shifted maximum around 198 nm suggest that, although alamethicin helices remain more inserted than surface bound, the alamethicin helices are in a more tilted state intermediate between the fully inserted and surface bound states of alamethicin. A supercoiled or funnel shaped channel structure could explain the observed spectra.[36,83]

3.3. Permeabilizing Properties of the Conjugates. To examine the ability of the scaffolded Alm to permeabilize DOPC vesicles, we used the calcein-release assay in which calcein is entrapped within vesicles at a concentration high enough to cause self-quenching of its fluorescence.[88] Permeabilization of vesicles, leading to calcein release into the exterior, dilutes the calcein sufficiently to induce a strong increase in fluorescence, which can be followed in real time. Complete release is accomplished by the addition of Triton X-100, allowing us to normalize data.

The kinetics of release of calcein varies significantly between Alm and the cyclodextrin constructs at comparable concentrations. The cyclodextrin linked alamethicin conjugates take up to 10-fold longer time than free alamethicin to reach a fluorescence plateau. (Figure 4A). The C-terminal polar part of alamethicin has been shown to be more flexible than the N-terminal part,[37] and one might expect that this would change the pore kinetics. Nevertheless, that is not the case. The reason for the slower kinetics of release for the scaffolded peptides could be that the well-defined pore geometry will slow down the release of calcein compared to the dynamic pore formed by Alm[92] and also that the calcein will have to pass through the hydrophobic lumen of the cyclodextrin ring.[93] However, in all cases, scaffolded alamethicin is significantly more efficient than free alamethicin on a mass basis (Figure 4B); the amount of peptide needed to effect 50% release is reduced 10-fold (relative to alamethicin alone) for the C-terminally linked conjugates and an impressive 100-fold for the N-terminally linked conjugates. When translated into molar ratios, we observe 50% release at a protein to lipid ratio >1/20000, making it highly likely that each Alm-CD construct constitutes an active pore forming unit. This ranking is observed in both zwitterionic and partially anionic lipids (see Figure S1, Supporting Information). Furthermore, the C-terminally linked alamethicins require higher peptide concentrations to permeabilize anionic vesicles. The preference for zwitterionic lipids has also previously been observed for the cationic AMPs pardaxin and novicidin.[67] However, we do not

dx.doi.org/10.1021/jp2098679 | J. Phys. Chem. B 2012, 116, 7652–7659

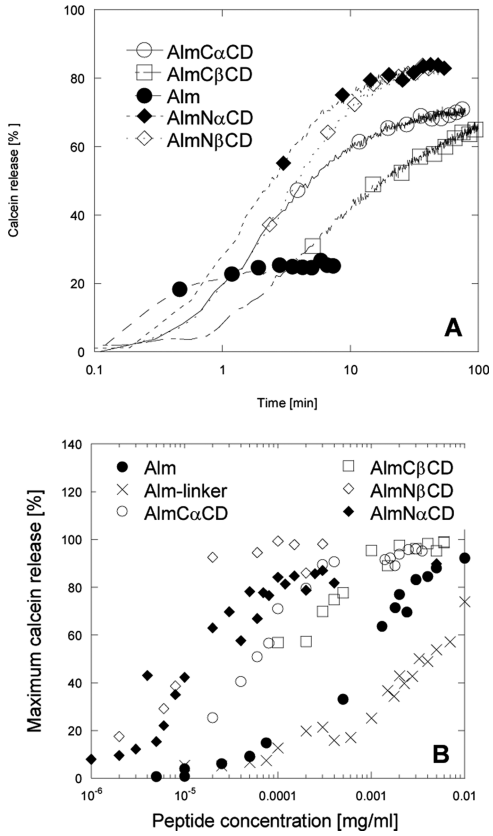

Figure 4. Calcein release assay. (A) Representative time profiles of calcein release by alamethicin and Alm:CD conjugates at ~0.1 μg/mL peptide. (B) The normalized maximum release of calcein from DOPC vesicles as a function of peptide concentration for alamethicin and derivatives. The peptide concentration represents alamethicin units, meaning that AlmCαCD and AlmNαCD contain 6 Alm units and AlmCβCD and AlmNβCD contain 7 Alm units.

observe this effect to the same extent with N-terminally linked alamethicins, suggesting that it is linked to the mode of insertion rather than the linking to cyclodextrin. These results support our initial assumption that less conjugated alamethicin is needed to permeate vesicles due to a higher local concentration of peptide. Nevertheless, the full-length alamethicin is a prerequisite for lysis since a βCD-scaffold coupled to the truncated peptide corresponding to residues 11−19 of alamethicin showed essentially no (0−3%) permeabilization of DOPC and 80% DOPC/20% DOPG vesicles. This clearly speaks in favor of the CD constructs working through a barrel stave mechanism as the shortened Alm constructs are not long enough to transverse the lipid bilayer, with only half of the 3.2 nm length of the wildtype.[94] This would also coinside with previous work by Huang and co-workers showing that alamethicin forms a pore through the barrel stave mechanism,[95] although other mechanisms in which peptides insert across the bilayer cannot be excluded on the basis of these experiments alone.

3.4. Ion-Channel Forming Properties of the Conjugates. To study the channel-forming ability of the alamethicin:CD conjugates and the conductive properties of the formed channels, we performed voltage-clamp studies. The dip-tip method was used to form the bilayer membrane on the tip of the micropipet.[68] The recording baseline was stable for at least 30 s, and the electrical noise in the recordings was significantly lower than current deflections. Significant differences were found between alamethicin and the alamethicin:CD conjugates (Figure 5). Previously, alamethicin has been shown to produce ion-channels

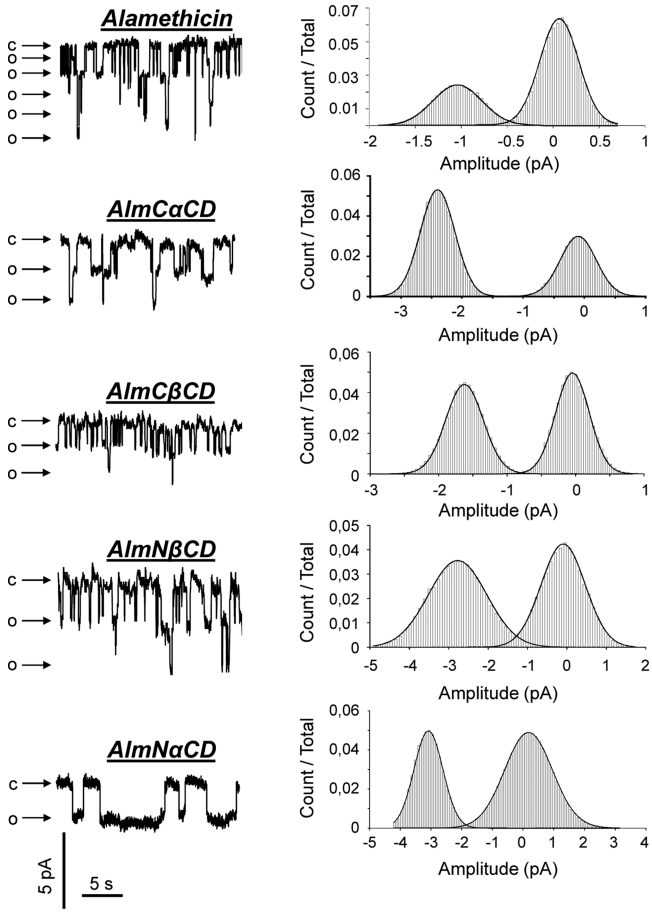

Figure 5. Single channel current recordings of alamethicin (10^{-3} mg/mL) and the alamethicin:CD conjugate (AlmCαCD, 10^{-3} mg/mL; AlmCβCD, 10^{-3} mg/mL; AlmNαCD, 10^{-5} mg/mL; AlmNβCD (13), 3×10^{-5} mg/mL) channels. Recordings were made at −40 mV; c = closed, and o = open.

with at least five well-defined conducting states each corresponding to different oligomeric states[11,20−23,25,26] in agreement with a mechanism involving expansion of an ion-channel (e.g., barrel-stave model) through insertion of additional helices into the channel wall. In contrast to the defined states of alamethicin, the alamethicin:CD conjugates produced longer lived channels with only one conductance state (Figure 5; multiples of only one conductance state are also shown). This shows that the use of the CD-scaffold and the ethylene glycol-linker allows for sufficient flexibility to permit the packing of the alamethicin helices necessary for channel formation. This is consistent with circular dichroism results (Figure 2B) showing that the secondary structure of the alamethicin:CD conjugates in solution were similar to the lipid-state structure.

Alamethicin did not produce any detectable conductance at peptide concentrations below 10^{-3} mg/mL. However, with the alamethicin:CD conjugates, conductance could be measured at concentrations as low as 10^{-5} mg/mL. This again supports our initial assumption that less of the conjugated peptide compared to the free alamethicin is needed to penetrate the membrane due to increased local concentration, as was also seen from the calcein release assays (Figure 4). Increasing the concentration of the N-

dx.doi.org/10.1021/jp2098679 | J. Phys. Chem. B 2012, 116, 7652−7659

terminal linked conjugates led to disintegration of the membrane, and therefore, studies were not done at concentrations higher than 3×10^{-5} M for AlmNαCD and 10^{-3} M for AlmNβCD. Whether this is a detergent-like effect or a more specific destruction of membrane on the pipet tip due to the increased number of alamethicin:CD conjugates remains unknown. Future studies employing the more stable lipid bilayer approach[89] could help to resolve this question.

Five well-defined conducting states were detected for alamethicin: first, 0.02 nS; second, 0.05 nS; third, 0.075 nS; fourth, 0.108 nS; and fifth, 0.15 nS. The single-channel conductance depends on the electrolyte concentrations, which complicates the direct comparison with other result. However, the currents measured at 150 mM KCl are comparable to previously measured currents at similar concentration and voltage.[44] In accordance to the barrel stave model, only one conducting state for alamethicin:CD conjugates should be possible. This is supported by the current study (Figure 5). The N-terminal linked conjugates formed the channels with the highest single channel conductance, as can also be judged from the slope of the current−voltage curve (Figure 6). A 0.083 nS and

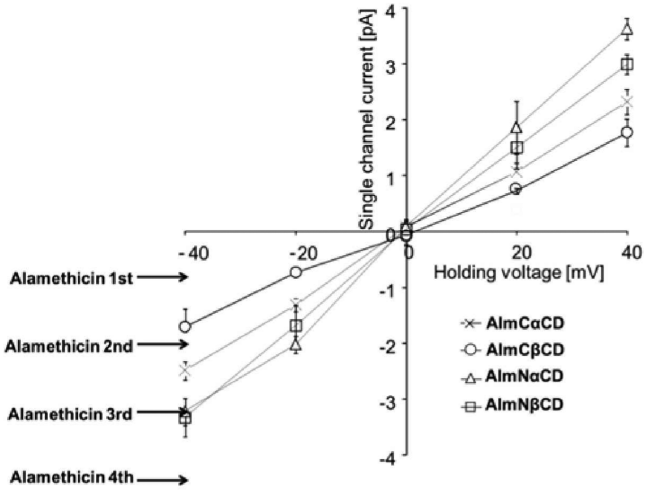

Figure 6. Conductance slopes for alamethicin and alamethicin:CD conjugates. The four lowest conductance states of alamethicin measured at −40 mV are shown.

0.080 nS conductance was measured for AlmNαCD and AlmNβCD, respectively. The amplitudes of the conductance's evoked by the N-terminal conjugates were significantly higher than those for the C-terminal conjugates. Surprisingly, the conductance induced by AlmCαCD, 0.062 nS, was considerably higher than the conductance of AlmCβCD, 0.043 nS.

Rectification of the channel current is typically seen for alamethicin at higher voltages due to the helix dipole.[44] In the current study, we observe linear voltage-dependences, hence no rectification, for alamethicin and alamethicin:CD conjugates between +40 mV and −40 mV (Figure 6). Such lack of voltage-dependence has also previously been observed for both alamethicin and other scaffolded alamethicin derivatives using low molar (<1 M) solution and relative low voltage.[38,48,53] The different conducting states observed for alamethicin at −40 mV are also depicted in Figure 6. It is generally believed that the lowest conductance state is a tetramer.[43,90] The conductance observed for the N-terminal linked conjugates resembles the third conducting state of alamethicin, whereas the conductance of the C-terminal linked conjugates resembles the second conducting state. The differences in conductance observed between N-terminal linked and C-terminal linked alamethicin must be due to structural differences. Oriented circular dichroism experiments also showed a more tilted state of α-helices for the N-terminal linked conjugates than the perpendicular helices observed for the C-terminal linked conjugates and alamethicin itself (Figure 3B). Clearly, there is a difference in the pore structure. However, whether it is due to different sizes of the channel pore or different electrical properties of the pore inner structure remain to be studied. Further studies are needed to deduce which channel resembles the natural alamethicin channel the most. This will furthermore enable us to link the different conducting states with the different oligomerization states. NMR experiments may ultimately provide more in-depth information about the exact structure of the different channels.

Interestingly, the current kinetics were different for the individual alamethicin:CD conjugates (Table 2, average lifetime).

Table 2. Average Lifetime and Open Propability

conjugate	average lifetime[a]	open propability[a]
alamethicin	67 ± 14 ms	0.35 ± 0.05 (3)
AlmCβCD	118 ± 11 ms	0.46 ± 0.04 (3)
AlmCαCD	156 ± 39 ms	0.60 ± 0.08 (6)
AlmNβCD	449 ± 123 ms	0.46 ± 0.02 (6)
AlmNαCD	1636 ± 942 ms	0.52 ± 0.04 (4)

[a]Measured at concentrations indicated in Figure 5.

Thus, an activated AlmNαCD channel remained open for a much longer time compared to the other conjugates. In fact, the AlmNαCD channel was able to remain open approximately 1.6 s in average. Also, the AlmNβCD channel had a long average lifetime of approximately 0.5 s, especially when using the high peptide concentrations. The shortest lifetime was detected for the nonmodified alamethicin having an average lifetime below 100 ms. Attaching alamethicin to CD clearly improves the lifetime of the channel being in the open state. The lifetime improvements are similar or better than previously reported. The open lifetime of a tetrameric ion-channel synthesized on a cyclic pseudopeptide has been reported to occasionally last more the one second.[52] Attaching alamethicin to a porphyrin-scaffold increased the average lifetime of the tetrameric ion-channel to approximately 5 s; however, the current levels were reported to be noisy.[53] Despite the different kinetics observed for the various alamethicin conjugates, the probability to stay open was not significantly different (Table 2, open probability).

The gating properties are clearly different between the two types of conjugates. The N-terminal linked conjugates, which also displayed a 10-fold greater efficiency in membrane permeabilization than the C-terminal linked conjugates, form channels with slow kinetics, whereas channels with fast kinetics are observed for the C-terminal linked conjugates. The presence of the only charged residue, Glu_{18}, near the C-terminal might influence the gating properties especially for the N-terminal linked conjugates. Furthermore, the C-terminal Glu_{18}−Gln_{19}−$Pheol_{20}$ residues have been suggested to form hydrogen bonds with the lipid head groups, thereby anchoring the helices to the lipid bilayer and contributing to the stabilization of the ion-channel.[91] This anchoring could contribute to the highly increased stability and lifetime observed for the channels formed by the N-terminal linked conjugates compared to the channels formed by the C-terminal linked conjugates. In addition, the

dx.doi.org/10.1021/jp2098679 | J. Phys. Chem. B 2012, 116, 7652−7659

overall shape of alamethicin ion-channels has been suggested to resemble that of a funnel; the N-terminal parts are in close contact, whereas the C-terminal parts are wider apart.[36] The two parts are connected by a helical kink formed by Pro_{14}. This arrangement allows for hydrogen bonding between Gln_7 residues of adjacent helices and enables the Glu_{18} residues to be sufficiently separated to avoid electrostatic repulsion. The CD-scaffold might favor such an arrangement when alamethicin is linked through the N-terminal. This could explain the different channel kinetics (Table 2) and the different helical alignments observed in the oriented circular dichroism (Figure 3). Conjugates containing a prolonged linker are currently being synthesized in order to evaluate the influence of the linker-scaffold on the channel stability.

4. CONCLUSIONS

In summary, the channel-forming peptide alamethicin has been synthesized with an alkyne group linked to either the C- or N-terminal. The alkyne containing peptides were then attached to a cyclodextrin-scaffold by use of click chemistry. The membrane permeabilizing properties of the conjugates proved to be highly effective, and lysis experiments revealed a 100-fold increase in activity for the most active conjugate in comparison to the free peptide. Also, the ion-channel properties of the conjugates were highly improved. Lifetimes for being in the open state were significantly prolonged, especially the N-terminally linked conjugates formed ion-channels with impressive lifetimes. The observed single conductance state and predominantly inserted state of CD-Alm constructs in combination suggest that membrane perturbation occur through formation of ion-channels presumably (i.e., other models can not be excluded) though the barrel-stave mechanism as previously suggested for alamethicin.[11,20−23,25,26] Aimed at obtaining further insight into the detailed structure of the ion-channel, efforts are currently underway to examine in more detail the interactions of these conjugates by NMR methods. The synthesis of conjugates containing a prolonged linker is hoped to elucidate the influence of the linker-scaffold system on the channel stability.

■ ASSOCIATED CONTENT

Supporting Information

Experimental procedures, characterization of all compounds, and detailed descriptions of the different methods. This material is available free of charge via the Internet at http://pubs.acs.org.

■ AUTHOR INFORMATION

Corresponding Author

*(N.C.N.) Phone: +45 2899 2541. E-mail: ncn@inano.au.dk. (D.E.O.) Phone: +45 8715 5441. E-mail: dao@inano.au.dk. (T.S.) Phone: +45 8715 5968. E-mail: ts@chem.au.dk.

Notes

The authors declare no competing financial interest.

■ ACKNOWLEDGMENTS

We thank the Danish National Research Foundation, the Lundbeck Foundation, the Carlsberg Foundation, the iNANO-school and OChem Graduate School, and Aarhus University for generous financial support of this work. Dr. Søren V. Hoffmann is gratefully acknowledged for ongoing access to storage ring facilities and unstintingly generous technical and scientific support.

■ REFERENCES

(1) Hale, J. D.; Hancock, R. E. *Expert Rev. Anti-Infect. Ther.* **2007**, *5*, 951−959.
(2) Lohner, K.; Blondelle, S. E. *Comb. Chem. High Throughput Screening* **2005**, 238−255.
(3) Zasloff, M. *Nature* **2002**, *415*, 389−395.
(4) Brogden, K. A. *Nat. Rev. Microbiol.* **2005**, *3*, 238−250.
(5) Hamill, P.; Brown, K.; Jenssen, H.; Hancock, R. E. *Curr. Opin. Biotechnol.* **2008**, 628−636.
(6) van't Hof, W.; Veerman, E. C. I.; Helmerhorst, E. J.; Amerongen, A. V. N. *Biol. Chem.* **2001**, 597−619.
(7) Toke, O. *Pept. Sci.* **2005**, *80*, 717−735.
(8) Giuliani, A.; Pirri, G.; Nicoletto, S. *Cent. Eur. J. Biol.* **2007**, *2*, 1−33.
(9) Shai, Y.; Oren, Z. *Peptides* **2001**, *22*, 1629−1641.
(10) Yang, L.; Harroun, T. A.; Weiss, T. M.; Ding, L.; Huang, H. W. *Biophys. J.* **2001**, *81*, 1475−1485.
(11) Baumann, G.; Mueller, P. *J. Supramol. Struct.* **1974**, *2*, 538−557.
(12) Ludtke, S. J.; He, K.; Heller, W. T.; Harroun, T. A.; Yang, L.; Huang, H. W. *Biochemistry* **1996**, *35*, 13723−13728.
(13) Wimley, W. C. *ACS Chem. Biol.* **2010**, *5*, 905−917.
(14) Matsuzaki, K.; Murase, O.; Fujii, N.; Miyajima, K. *Biochemistry* **1996**, *35*, 11361−11368.
(15) Duclohier, H. *Chem. Biodiversity* **2007**, *4*, 1023−1026.
(16) Duclohier, H. *Curr. Pharm. Des.* **2010**, *16*, 3212−3223.
(17) Degenkolb, T.; von Döhren, H.; Fog Nielsen, K.; Samuels, G. J.; Brückner, H. *Chem. Biodiversity* **2008**, *5*, 671−680.
(18) Meyer, C. E.; Reusser, F. *Experientia* **1967**, *23*, 85−86.
(19) Gordon, L. G. M.; Haydon, D. A. *Biochim. Biophys. Acta, Biomembr.* **1972**, *255*, 1014−1018.
(20) Cafiso, D. S. *Annu. Rev. Biophys. Biomol. Struct.* **1994**, *23*, 141−165.
(21) Sansom, M. S. P. *Q. Rev. Biophys.* **1993**, *26*, 365−421.
(22) Leitgeb, B.; Szekeres, A.; Manczinger, L.; Vágvölgyi, C.; Kredics, L. *Chem. Biodiversity* **2007**, *4*, 1027−1051.
(23) Woolley, G. A.; Wallace, B. *J. Membr. Biol.* **1992**, *129*, 109−136.
(24) Whitmore, L.; Wallace, B. A. *Eur. Biophys. J.* **2004**, *33*, 233−237.
(25) Fox, R. O.; Richards, F. M. *Nature* **1982**, *300*, 325−330.
(26) Mathew, M. K.; Balaram, P. *FEBS Lett.* **1983**, *157*, 1−5.
(27) Bak, M.; Bywater, R. P.; Hohwy, M.; Thomsen, J. K.; Adelhorst, K.; Jakobsen, H. J.; Sørensen, O. W.; Nielsen, N. C. *Biophys. J.* **2001**, *81*, 1684−1698.
(28) Breed, J.; Biggin, P. C.; Kerr, I. D.; Smart, O. S.; Sansom, M. S. P. *Biochim. Biophys. Acta, Biomembr.* **1997**, *1325*, 235−249.
(29) Tieleman, D. P.; Hess, B.; Sansom, M. S. P. *Biophys. J.* **2002**, *83*, 2393−2407.
(30) Constantin, D.; Brotons, G.; Jarre, A.; Li, C.; Salditt, T. *Biophys. J.* **2007**, *92*, 3978−3987.
(31) Hall, J. E.; Vodyanoy, I.; Balasubramanian, T. M.; Marshall, G. R. *Biophys. J.* **1984**, *45*, 233−247.
(32) He, K.; Ludtke, S. J.; Worcester, D. L.; Huang, H. W. *Biophys. J.* **1996**, *70*, 2659−2666.
(33) Pan, J.; Tristram-Nagle, S.; Nagle, J. *J. Membr. Biol.* **2009**, *231*, 11−27.
(34) Thøgersen, L.; Schiøtt, B.; Vosegaard, T.; Nielsen, N. C.; Tajkhorshid, E. *Biophys. J.* **2008**, *95*, 4337−4347.
(35) Salnikov, E. S.; Zotti, M. D.; Formaggio, F.; Li, X.; Toniolo, C.; O'Neil, J. D. J.; Raap, J.; Dzuba, S. A.; Bechinger, B. *J. Phys. Chem. B* **2009**, *113*, 3034−3042.
(36) Sansom, M. S. P. *Eur. Biophys. J.* **1993**, *22*, 105−124.
(37) Duclohier, H.; Wróblewski, H. *J. Membr. Biol.* **2001**, *184*, 1−12.
(38) Mak, D. O.; Webb, W. W. *Biophys. J.* **1995**, *69*, 2323−2336.
(39) Vosegaard, T.; Bertelsen, K.; Pedersen, J. M.; Thøgersen, L.; Schiøtt, B.; Tajkhorshid, E.; Skrydstrup, T.; Nielsen, N. C. *J. Am. Chem. Soc.* **2008**, *130*, 5028−5029.
(40) Bertelsen, K.; Paaske, B.; Thøgersen, L.; Tajkhorshid, E.; Schiøtt, B.; Skrydstrup, T.; Nielsen, N. C.; Vosegaard, T. *J. Am. Chem. Soc.* **2009**, *131*, 18335−18342.

(41) Dittmer, J.; Thøgersen, L.; Underhaug, J.; Bertelsen, K.; Vosegaard, T.; Pedersen, J. M.; Schiøtt, B.; Tajkhorshid, E.; Skrydstrup, T.; Nielsen, N. C. *J. Phys. Chem. B* **2009**, *113*, 6928−6937.
(42) Woolley, G. A. *Chem. Biodiversity* **2007**, *4*, 1323−1337.
(43) You, S.; Peng, S.; Lien, L.; Breed, J.; Sansom, M. S. P.; Woolley, G. A. *Biochemistry* **1996**, *35*, 6225−6232.
(44) Woolley, G. A.; Biggin, P. C.; Schultz, A.; Lien, L.; Jaikaran, D. C.; Breed, J.; Crowhurst, K.; Sansom, M. S. *Biophys. J.* **1997**, *73*, 770−778.
(45) Duclohier, H.; Kociolek, K.; Stasiak, M.; Leplawy, M. T.; Marshall, G. R. *Biochim. Biophys. Acta, Biomembr.* **1999**, *1420*, 14−22.
(46) Starostin, A. V.; Butan, R.; Borisenko, V.; James, D. A.; Wenschuh, H.; Sansom, M. S. P.; Woolley, G. A. *Biochemistry* **1999**, *38*, 6144−6150.
(47) Sakoh, M.; Okazaki, T.; Nagaoka, Y.; Asami, K. *Biochim. Biophys. Acta, Biomembr.* **2003**, *1612*, 117−121.
(48) Okazaki, T.; Sakoh, M.; Nagaoka, Y.; Asami, K. *Biophys. J.* **2003**, *85*, 267−273.
(49) Okazaki, T.; Nagaoka, Y.; Asami, K. *Bioelectrochemistry* **2007**, *70*, 380−386.
(50) Noshiro, D.; Asami, K.; Futaki, S. *Biophys. J.* **2010**, *98*, 1801−1808.
(51) Duclohier, H.; Alder, G.; Kociolek, K.; Leplawy, M. T. *J. Pept. Sci.* **2003**, *9*, 776−783.
(52) Matsubara, A.; Asami, K.; Akagi, A.; Nishino, N. *Chem. Commun.* **1996**, 2069−2070.
(53) Wassner, A. J.; Hurt, J. A.; Lear, J. D.; Åkerfeldt, K. S. *Org. Lett.* **2002**, *4*, 1647−1649.
(54) Jaikaran, D. C. J.; Biggin, P. C.; Wenschuh, H.; Sansom, M. S. P.; Woolley, G. A. *Biochemistry* **1997**, *36*, 13873−13881.
(55) Futaki, S.; Fukuda, M.; Omote, M.; Yamauchi, K.; Yagami, T.; Niwa, M.; Sugiura, Y. *J. Am. Chem. Soc.* **2001**, *123*, 12127−12134.
(56) Kiwada, T.; Sonomura, K.; Sugiura, Y.; Asami, K.; Futaki, S. *J. Am. Chem. Soc.* **2006**, *128*, 6010−6011.
(57) Jung, G.; Redemann, T.; Kroll, K.; Meder, S.; Hirsch, A.; Boheim, G. *J. Pept. Sci.* **2003**, *9*, 784−798.
(58) Woolley, G. A.; Epand, R. M.; Kerr, I. D.; Sansom, M. S. P.; Wallace, B. A. *Biochemistry* **1994**, *33*, 6850−6858.
(59) Mutter, M. *Trends Biochem. Sci.* **1988**, *13*, 260−265.
(60) Mutter, M.; Vuilleumier, S. *Angew. Chem., Int. Ed.* **1989**, *28*, 535−554.
(61) Tornøe, C. W.; Christensen, C.; Meldal, M. *J. Org. Chem.* **2002**, *67*, 3057−3064.
(62) Rostovtsev, V. V.; Green, L. G.; Fokin, V. V.; Sharpless, K. B. *Angew. Chem., Int. Ed.* **2002**, *41*, 2596−2599.
(63) Himo, F.; Lovell, T.; Hilgraf, R.; Rostovtsev, V. V.; Noodleman, L.; Sharpless, K. B.; Fokin, V. V. *J. Am. Chem. Soc.* **2005**, *127*, 210−216.
(64) Bock, V. D.; Hiemstra, H.; van Maarseveen, J. H. *Eur. J. Org. Chem.* **2006**, *2006*, 51−68.
(65) Meldal, M.; Tornøe, C. W. *Chem. Rev.* **2008**, *108*, 2952−3015.
(66) Nielsen, S. B.; Otzen, D. E. *J. Colloid Interface Sci.* **2010**, *345*, 248−256.
(67) Vad, B.; Thomsen, L. A.; Bertelsen, K.; Franzmann, M.; Pedersen, J. M.; Nielsen, S. B.; Vosegaard, T.; Valnickova, Z.; Skrydstrup, T.; Enghild, J. J.; Wimmer, R.; Nielsen, N. C.; Otzen, D. E. *Biochim. Biophys. Acta, Proteins Proteomics* **2010**, *1804*, 806−820.
(68) Coronado, R.; Latorre, R. *Biophys. J.* **1983**, *43*, 231−236.
(69) Khan, A. R.; Forgo, P.; Stine, K. J.; D'Souza, V. T. *Chem. Rev.* **1998**, *98*, 1977−1996.
(70) Tabushi, I.; Kuroda, Y.; Yokota, K. *Tetrahedron Lett.* **1982**, *23*, 4601−4604.
(71) Pregel, M. J.; Jullien, L.; Canceill, J.; Lacombe, L.; Lehn, J.-M. *J. Chem. Soc., Perkin Trans. 2* **1995**, 417−426.
(72) Madhavan, N.; Robert, E. C.; Gin, M. S. *Angew. Chem., Int. Ed.* **2005**, *44*, 7584−7587.
(73) Chui, J. K. W.; Fyles, T. M. *Chem. Commun.* **2010**, *46*, 4169−4171.
(74) Bayley, H.; Jayasinghe, L. *Mol. Membr. Biol.* **2004**, *21*, 209−220.
(75) Li, W.-W.; Claridge, T. D. W.; Li, Q.; Wormald, M. R.; Davis, B. G.; Bayley, H. *J. Am. Chem. Soc.* **2011**, *133*, 1987−2001.
(76) Luo, Y.; Egwolf, B.; Walters, D. E.; Roux, B. T. *J. Phys. Chem. B* **2009**, *114*, 952−958.
(77) Gu, L.-Q.; Bayley, H. *Biophys. J.* **2000**, *79*, 1967−1975.
(78) Gu, L.-Q.; Cheley, S.; Bayley, H. *Science* **2001**, *291*, 636−640.
(79) Gadelle, A.; Defaye, J. *Angew. Chem., Int. Ed.* **1991**, *30*, 78−80.
(80) Ashton, P. R.; Königer, R.; Stoddart, J. F.; Alker, D.; Harding, V. D. *J. Org. Chem.* **1996**, *61*, 903−908.
(81) Srinivasachari, S.; Fichter, K. M.; Reineke, T. M. *J. Am. Chem. Soc.* **2008**, *130*, 4618−4627.
(82) Hjørringgaard, C. U.; Pedersen, J. M.; Vosegaard, T.; Nielsen, N. C.; Skrydstrup, T. *J. Org. Chem.* **2009**, *74*, 1329−1332.
(83) Woolley, G. A.; Wallace, B. A. *Biochemistry* **1993**, *32*, 9819−9825.
(84) Schwarz, G.; Stankowski, S.; Rizzo, V. *Biochim. Biophys. Acta, Biomembr.* **1986**, *861*, 141−151.
(85) Hunt, J. F.; Rath, P.; Rothschild, K. J.; Engelman, D. M. *Biochemistry* **1997**, *36*, 15177−15192.
(86) Winston, P. W.; Bates, D. H. *Ecology* **1960**, *41*, 232−237.
(87) Wu, Y.; Huang, H. W.; Olah, G. A. *Biophys. J.* **1990**, *57*, 797−806.
(88) Allen, T. M.; Cleland, L. G. *Biochim. Biophys. Acta, Biomembr.* **1980**, *597*, 418−426.
(89) Sondermann, M.; George, M.; Fertig, N.; Behrends, J. C. *Biochim. Biophys. Acta, Biomembr.* **2006**, *1758*, 545−551.
(90) Asami, K.; Okazaki, T.; Nagai, Y.; Nagaoka, Y. *Biophys. J.* **2002**, *83*, 219−228.
(91) Tieleman, D. P.; Berendsen, H. J. C.; Sansom, M. S. P. *Biophys. J.* **1999**, *76*, 1757−1769.
(92) Hall, J. E.; Vodyanoy, I.; Balasubramanian, T. M.; Marshall, G. R. *Biophys. J.* **1984**, *45*, 233−247.
(93) Vyas, A.; Saraf, S.; Saraf, S. *J. Inclusion Phenom. Macrocyclic Chem.* **2008**, *62*, 23−42.
(94) Ionov, R.; El-Abed, A.; Angelova, A.; Goldmann, M.; Peretti, P. *Biophys. J.* **2000**, *78*, 3026−3035.
(95) Qian, S.; Wang, W.; Yang, L.; Huang, H. W. *Biophys. J.* **1998**, *94*, 3512−3522.